



ELSEVIER

Contents lists available at ScienceDirect

Mechanical Systems and Signal Processing

journal homepage: www.elsevier.com/locate/ymssp

Optimal negative derivative feedback controller design for collocated systems based on H_2 and H_∞ method

Rasa Jamshidi^{a,b,*}, Christophe Collette^{a,b}^a BEAMS Department, Université Libre de Bruxelles, Belgium^b Department of Aerospace and Mechanical Engineering, Université de Liège, Belgium

ARTICLE INFO

Communicated by H. Ouyang

Keywords:

Negative derivative feedback (NDF)
 Collocated system
 Band-pass filter
 Vibration mitigation
 Maximum damping
 Pole-zero pattern

ABSTRACT

In this paper, a direct procedure is presented in order to design negative derivative feedback (NDF) controller for collocated systems. Collocated systems have embedded sensors and actuators, which have an alternating poles and zeroes in frequency domain, which creates asymptotic stability. NDF is a band-pass filter, cutting off the control action far from the natural frequencies associated with the controlled modes, which reduces the spillover effect. Since it is a band-pass filter, it can effectively control the lower and higher frequency disturbances. Also, it is very efficient controller for higher frequencies' vibration mitigation. An approach for an optimal design of NDF controller to implement on collocated system is presented. A simple, collocated system is considered and a mode of it is targeted to damp. Maximum damping method is used to extract all of the controller constants dependent on closed-loop damping value. Afterward, H_2 and H_∞ methods are utilized to determine the closed-loop damping value optimally. The results show that NDF not only can easily damp the targeted mode impactfully but also can reduce some level of vibrations in the modes after that as well. This shows the power of NDF filter on vibration mitigation of modes located in a band of frequency. The proposed method is applicable for any general system and for any zero/pole patterns of collocated system, easily. It can be applied for any collocated system with zero before pole pattern or zero after pole pattern.

1. Introduction

In the past decade, by introducing new ways of production, the weight and consequently internal damping of structures have been decreased enormously. The benefit of using lightweight structures in engineering applications, is lessening the energy consumption. On the other side, using lightweight structures with low internal structural damping, causes higher levels of vibration, specially around the structure's natural frequency. Therefore, the necessity of vibration attenuation applications on this structure has been enlarged exponentially, in the past decade. For this end, researchers are looking for effective techniques which can provide a sufficient force to damp a targeted mode without destabilizing other modes.

Recently, applying embedded sensors and actuators on lightly damped structures, has increased enormously. In this way, the structure's vibration is damped actively. It has been shown that the use of collocated actuator and sensor, for a lightly damped flexible structure, always leads to alternating poles and zeros near the imaginary axis. This property guarantees the asymptotic stability, even if the system parameters are subject to large perturbations. This is because the root locus plot keeps the same general shape, and remains entirely within the left half plane when the system parameters are changed from their nominal values. Such a control system is said to

* Corresponding author.

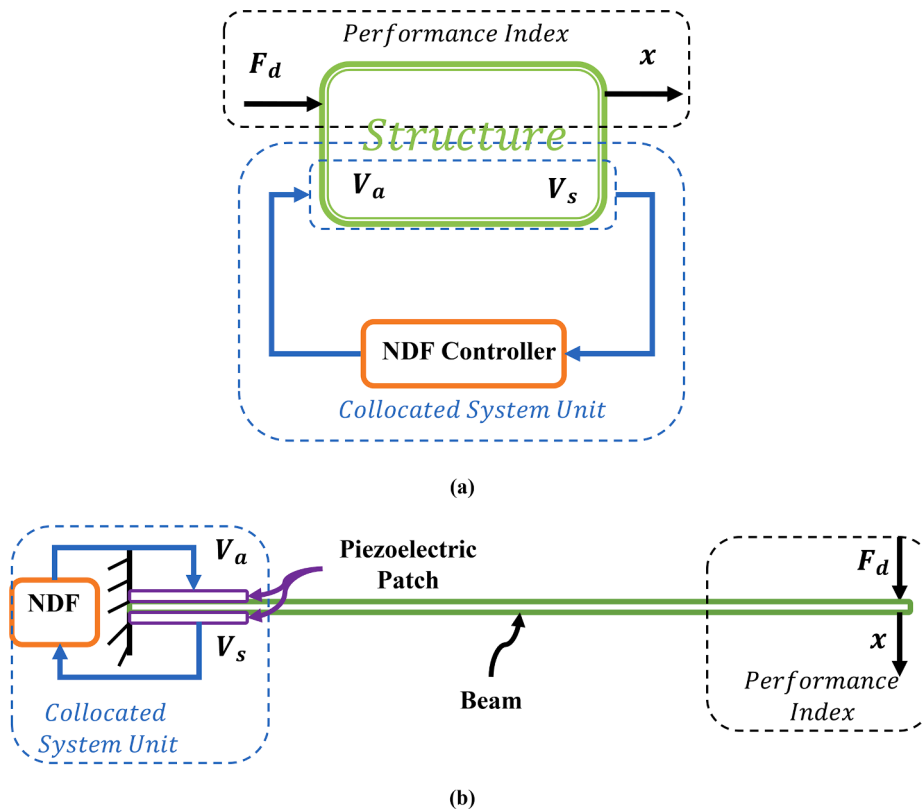


Fig. 1. a) Schematic diagram of collocated systems applying NDF controller b) A simple beam with collocated Piezoelectric patches and NDF controller considering tip displacement to tip force $\frac{x}{F_d}$ as a Performance Index.

be robust with respect to stability. The use of collocated actuator/sensor pairs is recommended whenever it is possible [1].

The most important factor in active vibration attenuation in collocated systems is utilizing an appropriate controller with high power to damp the vibration, impeccably. There are a wide range of control laws can be used for this purpose such as direct velocity feedback [2], integral force feedback [3], digital shunt absorber [4], positive position feedback [5], Active mass damper [8], integral force feedback controller [9]. While each of these control laws have its own upsides, there are some restrictions for each of them which avoid them to be used in many applications. Therefore, in many conditions, many of these control laws are not appropriate at all. For instance, positive position feedback (PPF) is a low-pass filter, which is very sensitive to low-frequency disturbances [6,7]. Applying PPF creates a static error from zero frequency to the targeted mode, which is an unsettling issue and can cause increase in the vibration level at lower frequencies. This issue makes PPF an inappropriate choice for targeting higher frequency modes.

To overcome the imperfections of mentioned techniques, Cazzulani [10] proposed a new resonant control logic which is called as negative derivative feedback (NDF) control, for the first time. The NDF is more robust than other logics with respect to the spillover effects and by acting as a band-pass filter, it cuts off both the higher and lower uncontrolled modes' contribution. This means that the controller dose not have downside effects on lower and higher modes. NDF showed better performance with respect to all the other techniques, both in terms of achieved damping and robustness to low- and high-frequency noises. Then, Cola [11] proposed an algorithm for designing NDF using output feedback control optimal method. The procedure was too complicated and not straightforward and hard to implement.

Syed [12] compared PPF and NDF performance on vibration control of a flexible arm featuring piezoelectric actuator. It was shown that NDF controller is more effective than PPF controller in terms of performance measures. Ripamonti [13], developed an adaptive NDF modal control algorithm, based on output feedback control method and applied it on a carbon fiber plate. The proposed algorithm is hard to apply on any system. Debattisti [14], evaluated distributed wireless-based control strategy through selective negative derivative feedback algorithm.

These various controllers can be applied to any structure to reduce undesired vibration. For example, for vibration reduction of conical shells there are many related articles in which piezoelectric patches with different distributions used [15–20].

Also, another way of damping the vibration of structures is using shunting piezoelectric patches. Many researchers developed different methods for this purpose [21–25]. The biggest downside of this method is the fact that the amplitude of vibration reduction is not considerable. Therefore, it is better to consider active methods to damp the vibration of structures. There are considerable number of articles [26–32] about damping vibration of structures actively using piezoelectric patches for sensing the displacement of structure and actuating on it.

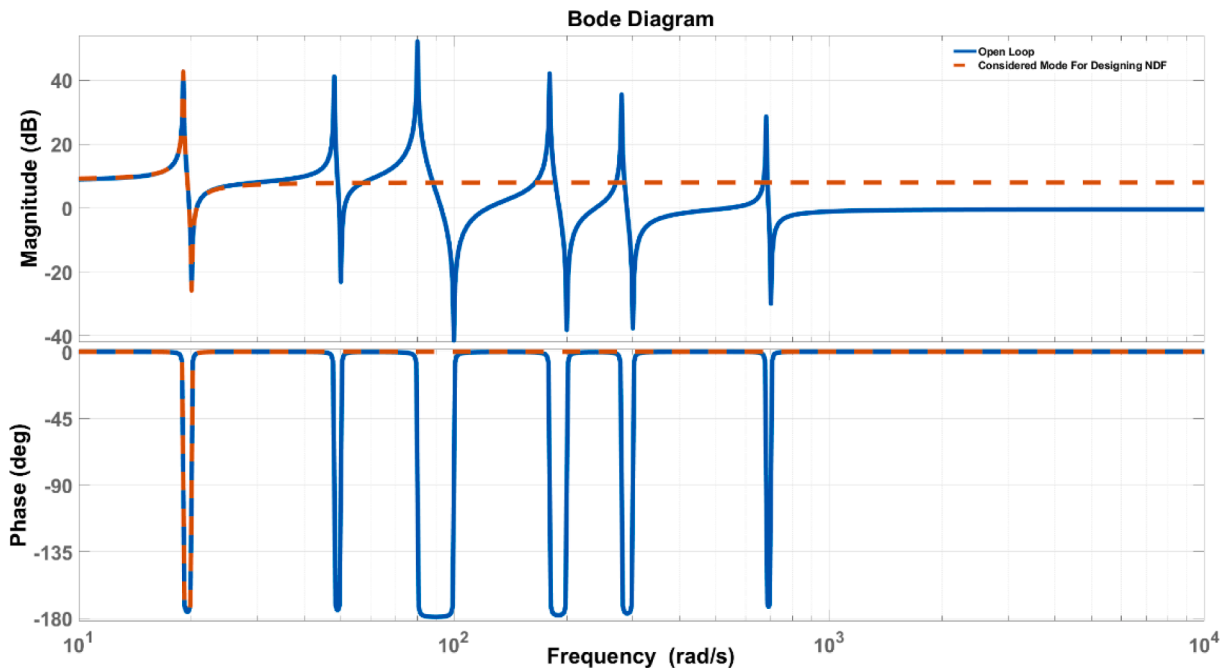


Fig. 2. Open-Loop of Collocated system with the first mode considered to damp by designing a NDF controller.

In Overall, the NDF controller is a new method which has not been studied deeply and also an optimal way for determining the controller parameters has not been presented, yet. Therefore, in this study, a careful consideration is taken in order to tune the parameters of the controller for collocated systems to get an optimal performance for a targeted mode without creating any undesired destabilizing issues on other modes or frequency ranges.

In this article, a straightforward method is presented to design NDF filter for collocated systems, optimally. To this end, first a simple collocated plant is considered and a mode in the open-loop is targeted to damp. Afterwards, the candidates of the poles of the NDF filter which can create maximum closed-loop damping are selected by the maximum damping method. In order to choose optimally, between these proposed candidates, H_2 and H_∞ optimization methods are utilized. The optimal closed-loop damping value is determined by two methods. Consequently, to meet the maximum damping method requirements, the NDF parameters are extracted in both of optimization methods. The designed NDF controller by this way, not only can easily damp the vibration of targeted mode impactfully, but also can decrease some vibration levels in the modes in the vicinity of targeted mode which is highly favorable. The presented method can be applied on any collocated system, for both zero before pole and zero after pole patterns. This shows the high applicability and execution capability of the proposed method in designing the NDF controller for any system. To verify the extracted method, the optimal NDF is applied to a beam in an experiment. The results show that optimal NDF is highly powerful in terms of vibration attenuation. Therefore, it is strongly recommended to choose the NDF controller for any vibration mitigation application, especially for lightly damped structures. For more clarifications, the performance of NDF is compared with PPF controller in an experiment. It has been shown that the performance of NDF is higher than PPF in the targeted mode. Also, the NDF can damp the modes close to the targeted mode, while PPF has not any effect on these mode at all. Therefore, it has been proven that the performance of NDF on vibration damping of collocated systems is higher than PPF.

2. Collocated systems

In this section, a collocated plant is considered for applying the NDF controller. A schematic block diagram of considered plant is presented in the Fig. 1.a. In this system, the disturbance force (F_d) is considered as an input and a displacement (x) is considered as an output. The frequency response between the output and disturbance input is regarded as a performance index of the system. In order to decrease the displacement (and consequently the performance index) of the system in the modes of system, an embedded collocated plant, including a sensor and an actuator are considered and a NDF controller is used to magnify the sensor signal and apply it on the actuator in an opposite direction. By this way, the displacement of the system will decrease actively.

As an example for collocated systems, in Fig. 1.b a typical collocated system, a beam with two embedded piezoelectric patches is shown. This is a representative of a large class of structures controlled with piezoelectric patches. Typically, one piezoelectric patch is used as sensor and the other one as an actuator on the structure. Both of them are placed at the same position on the beam, in order to make collocated poles and zeros in open-loop frequency response which has no roll off at high frequencies. In such cases, the source of disturbances usually comes from external force F_d injected somewhere on the structure (In the beam, usually the tip force is considered as disturbance force). The motion of structure (x) is mainly measured at the position where the maximum displacement of desired

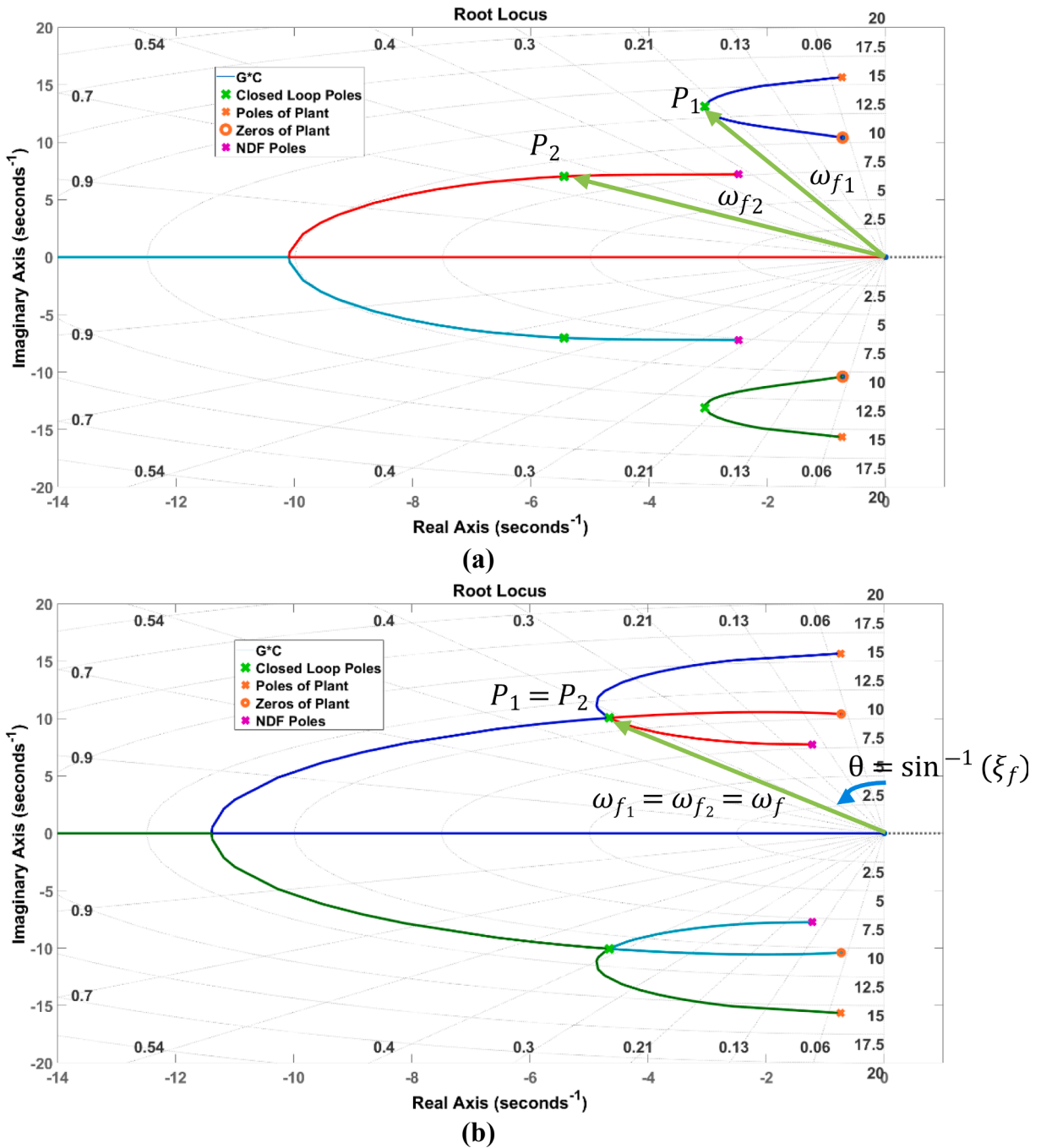


Fig. 3. Root-Locus curve for the case of a) non-merged, b) merged poles of closed-loop.

mode happens (Also, usually the tip displacement is considered as a motion of beam).

The collocated transfer function between actuator signal (V_a) and sensor signal (V_s) is the transfer function of interest which is used for designing the NDF controller. After designing the controller and closing the loop, the performance index is measured and compared with the condition where there is no control.

The open-loop of collocated systems are presented in Fig. 2. Tuning the parameters of NDF only depends on the information of the target mode. Although the frequency response of the corresponding structure has an infinite number of resonance frequencies, the design of optimal NDF is focused only on the target resonance which is aimed to be damped (Fig. 2). It is worth to mention that NDF does not destabilize the higher modes due to a good roll-off. The open-loop transfer function of interest is regarded as model and shown in Fig. 2 when the first resonance frequency is targeted to damp. The effect of residual modes is also considered automatically in this

way when the magnitude of the model in low frequencies is chosen the same as the magnitude of the general model.

The use of collocated (and dual) actuator and sensor pairs, for a lightly damped flexible structure, always leads to alternating poles and zeros near the imaginary axis, in the root locus plot. This interlacing property is used to develop Single Input-Single Output (SISO) active damping schemes with guaranteed stability. The pole and zero in the collocated systems have imaginary and real parts [1]. Consequently, the model can be defined in Laplace form as a transfer function between V_a and V_s :

$$G(s) = \frac{V_a}{V_s} = g_0 \frac{s^2 + 2\xi_z \omega_z s + \omega_z^2}{s^2 + 2\xi_p \omega_p s + \omega_p^2} \quad (1)$$

where ω_p and ξ_p are the frequency and damping ratio of pole and, similarly, ω_z and ξ_z are the frequency and damping ratio of zero of the system, respectively. Also, g_0 is the constant which includes the residual modes. So, Eq. (1) represents the transfer function of targeted mode in the open-loop (Fig. 2) which is considered as a model. In the following steps, a procedure for designing an optimal NDF for the model, is presented.

3. Maximum damping

In this section, maximum damping method is utilized to extract the candidates of the NDF controller's parameters. First the NDF controller transfer function is considered as [10]:

$$C(s) = -\frac{K_c \omega_c s}{s^2 + 2\xi_c \omega_c s + \omega_c^2} \quad (2)$$

where K_c , ξ_c , and ω_c are the gain, damping ratio and cutoff frequency of the controller. Considering the plant transfer function (Eq. (1)) and the NDF controller (Eq. (2)), the characteristic equation of the closed-loop function is extracted and presented in Eq. (3).

$$s^4 + (2\xi_p \omega_p + 2\xi_c \omega_c + k_c \omega_c g_0) s^3 + (\omega_p^2 + \omega_c^2 + 4\xi_p \xi_c \omega_p \omega_c + 2\xi_z \omega_z K_c \omega_c g_0) s^2 + (2\xi_p \omega_p \omega_c^2 + 2\xi_c \omega_c \omega_p^2 + g_0 \omega_z^2 K_c \omega_c) s + \omega_p^2 \omega_c^2 = 0 \quad (3)$$

By Eq. (3), the location of the NDF poles can be determined. The design is focused on the right loop, which is between pole and zero of the plant (Fig. 3.a). The size of this loop (and consequently the performance of controller) is strongly dependent on the cutoff frequency and damping ratio of controller. In other words, the location of the NDF poles in regards with the pole and zero of the plant has a high impact on the performance of the controller. Based on maximum damping method, the best controller which gives maximum damping of closed-loop response is the one which can make the region of right loops in Fig. 3.a maximized. In this case, the feedback gain can be tuned in such a way that the angle of the asymptotic line of the closed-loop pole with respect to the imaginary axis is at highest level. Based on maximum damping method, this maximized loop occurs when the right loops are intersecting with the left loop (Fig. 3.b).

As it is shown in Fig. 3.b, for the merged poles of closed-loop, the frequency and damping ratio of the closed-loop are ω_f and ξ_f , respectively. In this condition, the characteristic equation of closed-loop system can be written in this form:

$$(s^2 + 2\xi_f \omega_f s + \omega_f^2)^2 = 0 \quad (4)$$

For simplifying, two non-dimensional parameters in regard with cutoff frequency of NDF (δ) and pole-zero pattern (λ) are introduced:

$$\delta = \frac{\omega_c}{\omega_p} \quad (5.a)$$

$$\lambda = \frac{\omega_z}{\omega_p} \quad (5.b)$$

In order to achieve maximum damping, Eq. (4) and (3) should be identical. Therefore, the polynomial coefficients of Eqs. (3) and (4) should be equivalent. For this end, four equations can be obtained, which are simplified and presented in Eq. (6).

$$2\xi_p \omega_p + 2\xi_c \omega_c + k_c \omega_c g_0 = 4\xi_f \omega_f \quad (6.a)$$

$$\omega_p^2 + \omega_c^2 + 4\xi_p \xi_c \omega_p \omega_c + 2\xi_z \omega_z K_c \omega_c g_0 = 4\xi_f^2 \omega_f^2 + 2\omega_f^2 \quad (6.b)$$

$$2\xi_p \omega_p \omega_c^2 + 2\xi_c \omega_c \omega_p^2 + g_0 \omega_z^2 K_c \omega_c = 4\xi_f \omega_f^3 \quad (6.c)$$

$$\omega_p^2 \omega_c^2 = \omega_f^4 \quad (6.d)$$

Considering Eqs. (6.d) and (5.a), it can be simply concluded that:

$$\omega_f = \sqrt{\delta} \omega_p \quad (7)$$

Eq. (7) defines the closed-loop poles' location relation with plant pole. By putting Eq. (7) into Eq. (6.b) and considering Eq. (5.b)

Table 1
Parameters of NDF controller for collocated system defined by maximum damping method.

δ	$(\xi_{eq} + 1) \pm \sqrt{\xi_{eq}^2 + 2\xi_{eq}}$
ξ_c	$\frac{(2\xi_f\sqrt{\delta} - \xi_p)(1 - \lambda^2) - (1 - \delta)[2\xi_f\sqrt{\delta} - \xi_p(1 + \delta)]}{\delta(1 - \lambda^2)}$
K_c	$\frac{2}{g_0} \frac{(1 - \delta)[2\xi_f\sqrt{\delta} - \xi_p(1 + \delta)]}{\delta(1 - \lambda^2)}$

and simplifying the attained equation, Eq. (8) is extracted.

$$\delta^2 - 2(\xi_{eq} + 1)\delta + 1 = 0 \tag{8}$$

where $\xi_{eq} = 2\xi_f^2 - 2\xi_p\xi_c - \xi_z\lambda K_c g_0$. Solving Eq. (8) will determine the value of δ , which represents the cutoff frequency parameters of the controller. Based on Eq. (8), δ is calculated as:

$$\delta = (\xi_{eq} + 1) - \sqrt{\xi_{eq}^2 + 2\xi_{eq}} \text{ (if } \delta < 1) \tag{9.a}$$

$$\delta = (\xi_{eq} + 1) + \sqrt{\xi_{eq}^2 + 2\xi_{eq}} \text{ (if } \delta > 1) \tag{9.b}$$

Based on Eq. (9), the cutoff frequency of the NDF filter can be located before ($\delta < 1$) or after ($\delta > 1$) the plant's pole. By inserting Eq. (5.a) and Eq. (7) into Eq. (6.a) and simplifying it, Eq. (10) is extracted.

$$\left(\xi_c + \frac{g_0}{2}K_c\right) = \frac{2\xi_f}{\sqrt{\delta}} - \frac{\xi_p}{\delta} \tag{10}$$

Similarly, by putting Eq. (5.a), (5.b) and Eq. (7) into Eq. (6.c) and simplifying the attained equation, Eq. (11) is extracted.

$$\left(\xi_c + \frac{g_0\lambda^2}{2}K_c\right) = 2\xi_f\sqrt{\delta} - \xi_p\delta \tag{11}$$

Clearly, Eqs. (10) and (11) are two equations with two unknown parameters (K_c and ξ_c). These parameters are extracted dependent on λ, δ, ξ_p and ξ_f and presented in Eqs. (12) and (13) respectively.

$$\xi_c = \frac{(2\xi_f\sqrt{\delta} - \xi_p)(1 - \lambda^2) - (1 - \delta)[2\xi_f\sqrt{\delta} - \xi_p(1 + \delta)]}{\delta(1 - \lambda^2)} \tag{12}$$

$$K_c = \frac{2}{g_0} \frac{(1 - \delta)[2\xi_f\sqrt{\delta} - \xi_p(1 + \delta)]}{\delta(1 - \lambda^2)} \tag{13}$$

By these equations, the parameters of NDF are extracted. For summary, these parameters are presented in the Table 1.

Table 1 determines the NDF controller's parameters by considering the maximum damping method. According to Table 1, the controller's parameters are defined by the closed-loop damping value (ξ_f) which varies from zero to one. Additionally, the parameters of controller (δ, ξ_c and K_c) are dependent on each other and cannot be calculated directly. That is because δ is dependent on ξ_c and K_c (Eq. (9)), and on the other hand, for calculating the ξ_c and K_c , the value of δ is needed (Eqs. (12) and (13)).

In order to solve these complicated equations, the extracted equations of ξ_c and K_c (Eqs. (12) and (13)) should be inserted into the extracted equation of δ (Eq. (9)). By this method, the magnitude of δ can be calculated easily for any value of closed-loop damping (ξ_f). Afterwards, the magnitude of ξ_c and K_c can be calculated easily for the considered value of closed-loop damping using Eqs. (12) and (13), respectively. Unfortunately, this equation cannot be solved analytically. Therefore, it should be carried out for each system numerically, separately for various value of closed-loop damping which varies from zero to one.

So, in this section, many candidates for the NDF controller, which all satisfy the requirements of merging poles, are extracted. These candidates are representative of closed-loop damping values varying from zero to one. Obviously, the higher closed-loop damping value is more appealing in vibration reduction. But higher closed-loop damping will come to a price of lower phase/gain or modulus margins. Therefore, there is a trade-off between performance and stability margins. To choose a reasonable choice between these candidates, an optimization method should be considered. To tackle this problem, two optimization algorithms (H_2 and H_∞) are considered and presented in the next section.

4. H_2 And H_∞ optimization method

In this section, optimization methods are considered in order to calculate an optimal value for closed-loop damping. After

Table 2
Parameters of NDF controller defined by maximum damping method in the condition of $\xi_p = 0, \xi_z = 0$

δ	$(2\xi_f^2 + 1) \pm 2\xi_f \sqrt{\xi_f^2 + 1}$
ξ_c	$\frac{2\xi_f(\delta - \lambda^2)}{\sqrt{\delta(1 - \lambda^2)}}$
K_c	$\frac{4\xi_f(1 - \delta)}{g_0 \sqrt{\delta(1 - \lambda^2)}}$

extracting the controller’s parameters based on the value of closed-loop damping, an optimal choice should be preferred for this value. In the optimization procedure, the main concentration can be the highest possible vibration reduction on the target mode without any concerns about other frequency ranges’ response (H_∞ method), or it can be about getting a logical amount of vibration reduction without any unsettling effects on other frequency ranges (H_2 method). For this end, H_2 and H_∞ algorithms are chosen to utilize. First, the norm that needed to be minimized is extracted. In this study, the closed-loop magnitude is considered as a norm to optimize. The closed-loop equation is extracted based on Eqs. (1) and (2).

$$\frac{G}{1 + GC} = \frac{g_0(s^2 + 2\xi_c \omega_c s + \omega_c^2)}{s^4 + (2\xi_p \omega_p + 2\xi_c \omega_c + k_c \omega_c g_0)s^3 + (\omega_p^2 + \omega_c^2 + 4\xi_p \xi_c \omega_p \omega_c + 2\xi_c \omega_c K_c \omega_c g_0)s^2 + (2\xi_p \omega_p \omega_c^2 + 2\xi_c \omega_c \omega_p^2 + g_0 \omega_c^2 K_c \omega_c)s + \omega_p^2 \omega_c^2}$$
(14)

For calculating the closed-loop system’s norm, $s = j\omega$ is inserted in the Eq. (14) and simplified and presented in Eq. (15).

$$\left| \frac{G}{1 + GC} \right| = \sqrt{\frac{(\omega_c^2 - \omega^2)^2 + (2\xi_c \omega_c \omega)^2}{(\omega^4 - (\omega_p^2 + \omega_c^2 + 2\xi_c \omega_c K_c \omega_c g_0)\omega^2 + \omega_p^2 \omega_c^2)^2 + (-(2\xi_p \omega_p + 2\xi_c \omega_c + g_0 K_c \omega_c)\omega^3 + (2\xi_p \omega_p \omega_c^2 + 2\xi_c \omega_c \omega_p^2 + g_0 \omega_c^2 K_c \omega_c)\omega)^2}}$$
(15)

Considering this norm, H_2 cost function and H_∞ cost functions can be calculated by:

$$H_2 = \int_0^\infty \sqrt{\frac{(\omega_c^2 - \omega^2)^2 + (2\xi_c \omega_c \omega)^2}{(\omega^4 - (\omega_p^2 + \omega_c^2 + 2\xi_c \omega_c K_c \omega_c g_0)\omega^2 + \omega_p^2 \omega_c^2)^2 + (-(2\xi_p \omega_p + 2\xi_c \omega_c + g_0 K_c \omega_c)\omega^3 + (2\xi_p \omega_p \omega_c^2 + 2\xi_c \omega_c \omega_p^2 + g_0 \omega_c^2 K_c \omega_c)\omega)^2}} d\omega$$
(16.a)

$$H_\infty = \sqrt{\frac{(\omega_c^2 - \omega^2)^2 + (2\xi_c \omega_c \omega)^2}{(\omega^4 - (\omega_p^2 + \omega_c^2 + 2\xi_c \omega_c K_c \omega_c g_0)\omega^2 + \omega_p^2 \omega_c^2)^2 + (-(2\xi_p \omega_p + 2\xi_c \omega_c + g_0 K_c \omega_c)\omega^3 + (2\xi_p \omega_p \omega_c^2 + 2\xi_c \omega_c \omega_p^2 + g_0 \omega_c^2 K_c \omega_c)\omega)^2}} \Big|_{\omega=\omega_p}$$
(16.b)

For obtaining the optimum value of the closed-loop damping, the cost function of H_2 or H_∞ should be calculated for each closed-loop damping value, separately. Afterwards, the minimum value of the calculated cost function represents the optimal value for the closed-loop damping of NDF. After defining the optimal closed-loop damping value, the parameters of the NDF controller are determined as well. Using H_∞ always lead to higher values of closed-loop damping. On the other hand, using H_2 always lead to higher stability margins.

It is worth mentioning, that the proposed algorithm for designing NDF controller, works for any pole-zero pattern in the open-loop (both zero before pole and zero after pole pattern in the system’s open-loop frequency response). This means that there are no restrictions of application in the pole-zero pattern in the open-loop of collocated system plant.

5. Stability

In this section, the stability of collocated plant with NDF controller is evaluated. For this purpose, the characteristic equation of the closed-loop system is considered (Eq. (3)). Since, there are many parameters in this equation, evaluating the stability becomes sophisticated. Therefore, a simplification is considered and the damping ratio of pole and zero of the plant, considered to be zero ($\xi_p = 0, \xi_z = 0$). The characteristic equation in this condition is presented in Eq. (17).

$$s^4 + (2\xi_c \omega_c + k_c \omega_c g_0)s^3 + (\omega_p^2 + \omega_c^2)s^2 + (2\xi_c \omega_c \omega_p^2 + g_0 \omega_c^2 K_c \omega_c)s + \omega_p^2 \omega_c^2 = 0$$
(17)

In this condition, the presented controller parameters considering maximum damping method in the Table 1 (parameters of NDF controller defined by maximum damping method), are simplified. These parameters are presented in the Table 2.

Table 3
Stability Criteria For NDF.

$\lambda < 1$	$\delta > \lambda^2$
$\lambda > 1$	$\delta < \lambda^2$

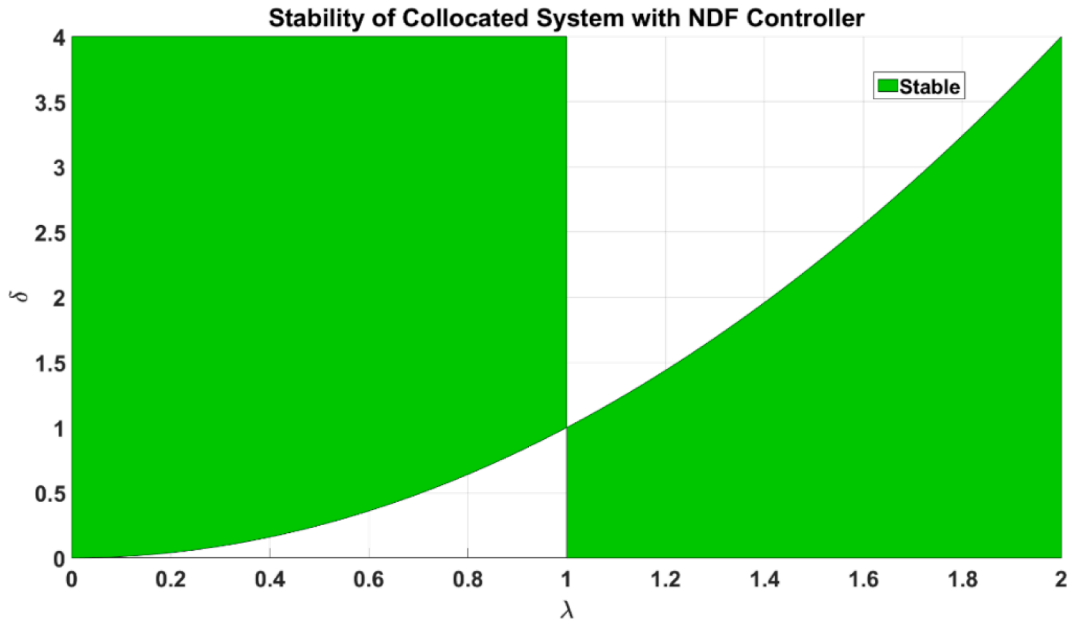


Fig. 4. Stable Areas of closed-loop system.

Table 4
Parameters of Zero before Pole Plant.

ξ_c	0.001
ξ_p	0.001
ω_z	10
ω_p	20
g	1

By determining the NDF’s parameters in Table 2, the controller parameters are calculated and inserted into Eq. (17). Based on Routh stability criterion, the conditions for closed-loop system to be stable are extracted and presented in Table 3. The stability of the system is dependent on cutoff frequency parameter of controller (δ) and the pole-zero pattern parameter (λ) of the plant. The result shows that the important factor for determining the stability of the system is the pole-zero pattern in the collocated system (λ). Whether it is zero before pole pattern ($\lambda < 1$) or zero after pole pattern ($\lambda > 1$), affects the stability of the closed-loop system impactfully. Therefore, having pole-zero pattern, the location of the cutoff frequency (δ parameter) should be determined wisely. The stability areas based two parameters of λ and δ are presented in the Fig. 4, for further clarifications.

Clearly, the stability criteria changes for a system with zero before pole pattern ($\lambda < 1$) to a system with zero after pole pattern ($\lambda > 1$), dramatically. However, for both of the systems, the controller cutoff frequency can be before pole ($\delta < 1$) or after pole ($\delta > 1$).

6. Practical examples

In order to clarify the presented method more vividly, in this section two practical examples are presented. The first example has a zero before pole pattern ($\lambda < 1$), and the second one has a zero after pole pattern ($\lambda > 1$) in the open-loop frequency response. Also, the robustness of presented algorithm is evaluated and the effect of uncertainties on the closed-loop damping value has been evaluated and discussed.

6.1. Zero before pole pattern

A collocated plant with zero before the pole pattern is considered in Eq. (18). Comparing Eq. (1) with Eq. (18), the parameters of

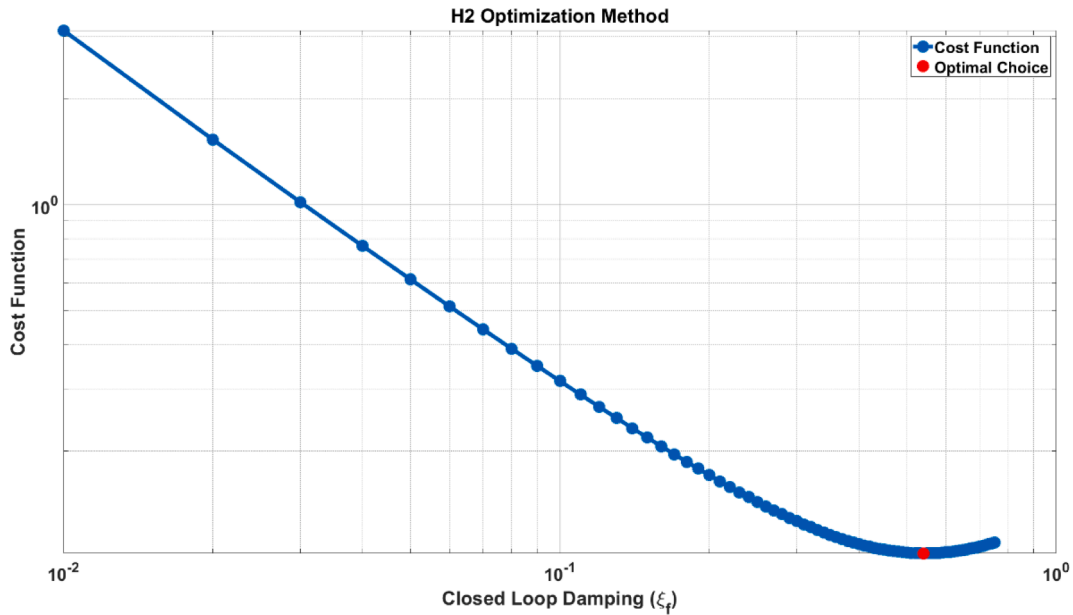


Fig. 5. The cost function of NDF controller based on H_2 for various closed-loop damping ($\lambda < 1$).

Table 5

Parameters of designed NDF controller (by H_2 & H_∞) with closed-loop damping value (ξ_f) ($\lambda < 1$).

	H_2	H_∞
ξ_f	0.5400	0.7400
ξ_c	0.2571	0.0153
ω_c	7.1279	5.0729
K_c	3.0984	5.8389

this plant are extracted and shown in Table 4.

$$G(s) = \frac{s^2 + 0.02*s + 100}{s^2 + 0.04*s + 400} \tag{18}$$

For this plant, two NDF controllers are designed and applied. In the first controller, the cutoff frequency is considered to be before pole ($\delta < 1$) and H_2 optimization method is utilized. The cost function of NDF controller based on H_2 optimization method for various closed-loop damping is shown in Fig. 5.

The minimum value of the cost function in Fig. 5 is chosen as an optimal choice for NDF controller. After calculating the optimal value for closed-loop damping, the parameters of the controller are calculated using Table 1. The designed controller’s parameters are extracted with H_2 method and shown in Table 5.

Bode diagram of the system in closed-loop condition in comparison with the system’s plant (open-loop) are presented in Fig. 6. The result shows that NDF filter damps the targeted mode magnificently without any imperfections.

The root locus of closed-loop system is also presented in Fig. 7 for further clarifications. Obviously, the closed-loop system has merging poles and poles of controller is chosen in such way that the closed-loop poles become merged. As mentioned in Table 4, the system damping without a controller is 0.001. In Fig. 7, the damping of closed-loop system (merging poles) is 0.54, which shows a high improvement in the structure’s damping. This vividly shows the power of NDF controller on increasing system damping (especially for low damped systems).

For the same system, the cost function of NDF controller based on H_∞ optimization method for various closed-loop damping is extracted as well. In this condition, there is no optimal choice and the maximum closed-loop possible is chosen and afterwards the controller’s parameters are defined and presented in the Table 5. The bode diagram and root locus of the closed-loop system considering this controller are shown in Fig. 8 and Fig. 9, respectively.

In Fig. 9, the damping of closed-loop system is 0.74, which shows a huge improvement in system damping. Comparing H_2 with H_∞ method, shows that H_∞ creates more damping in the closed-loop response. However, this comes to the price of creating a notch at the location of cutoff frequency (in the bode diagram (Fig. 8)) which is not desired. Therefore, in this case, H_2 method is more preferred. The results easily shows the power of NDF controller on damping increase of collocated systems with zero before pole pattern (especially low damped systems).

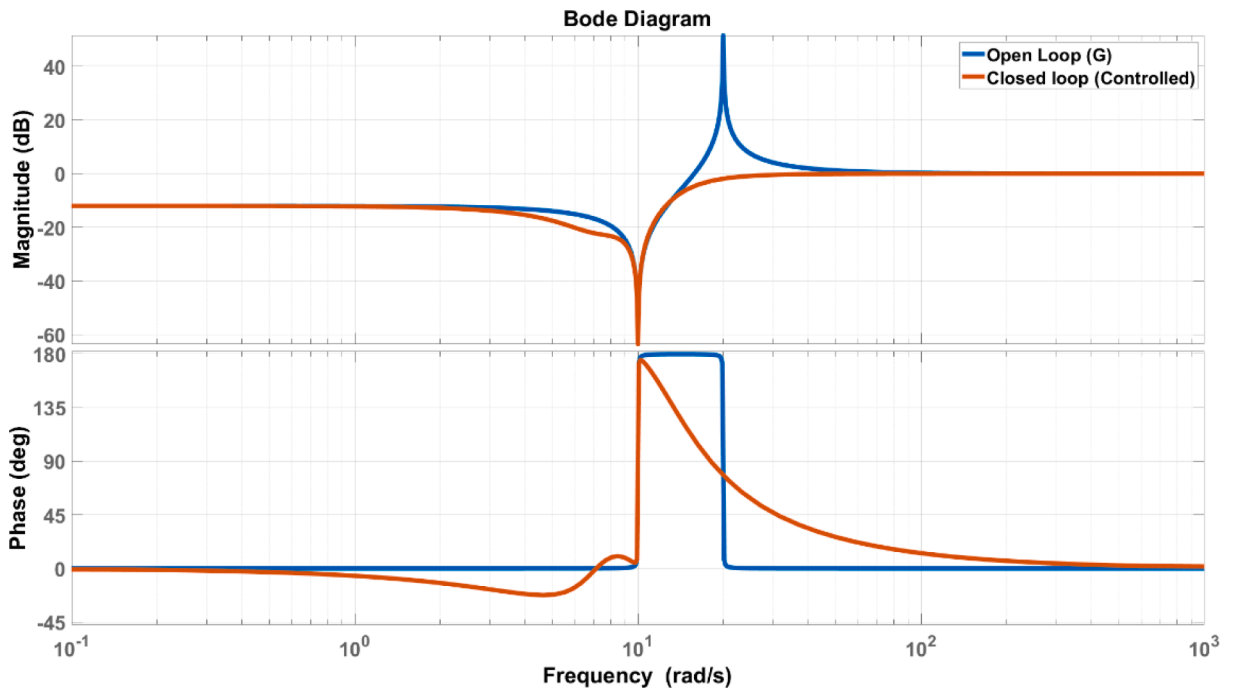


Fig. 6. Open-loop and closed-loop response of system based on H_2 ($\lambda < 1, \delta < 1$).

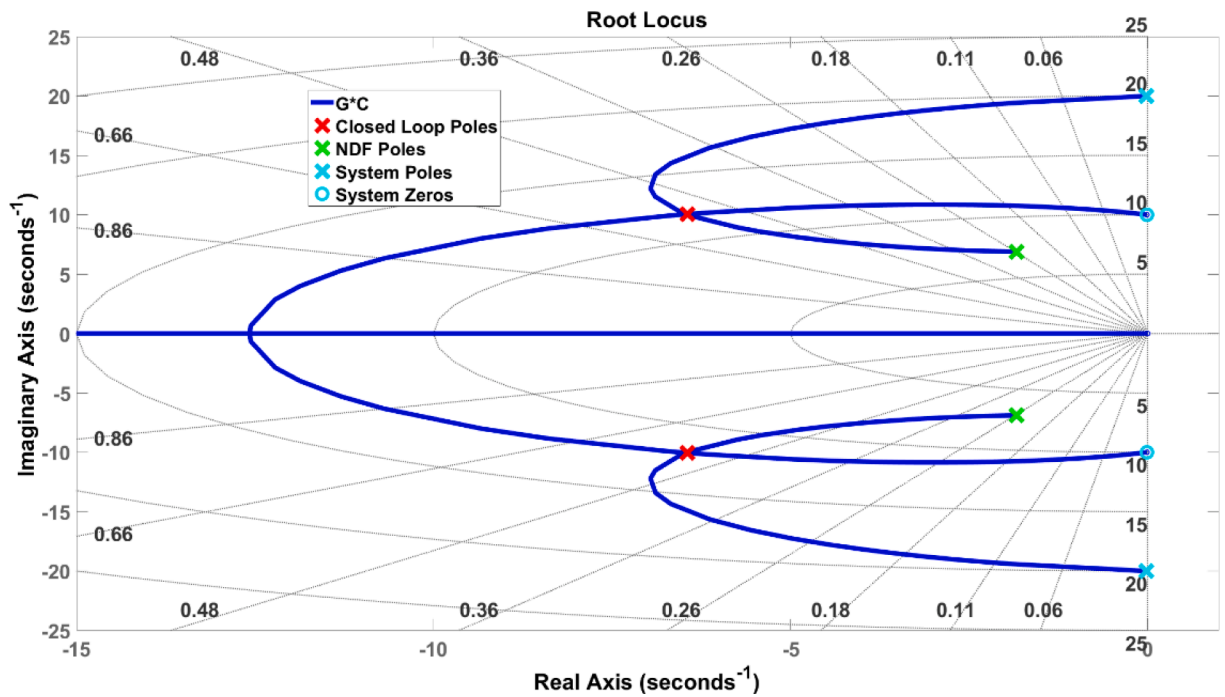


Fig. 7. Root Locus of the collocated system with NDF controller based on H_2 ($\lambda < 1, \delta < 1$).

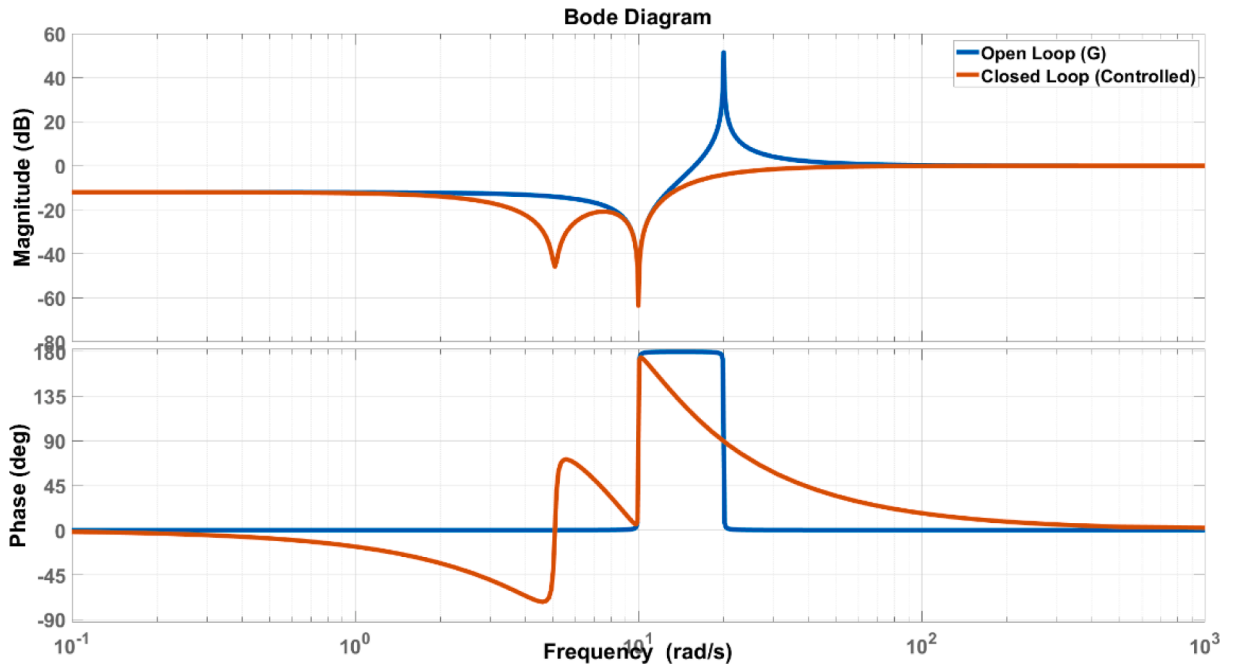


Fig. 8. Open-loop and closed-loop response of system based on H_∞ ($\lambda < 1, \delta < 1$).

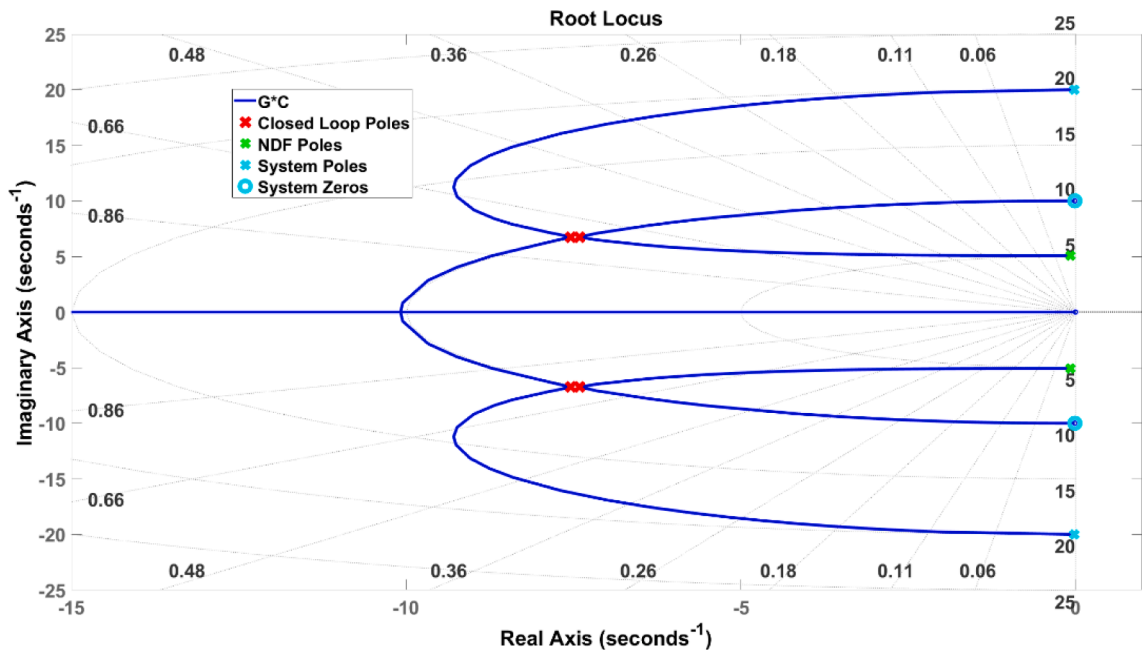


Fig. 9. Root Locus of the collocated system with NDF controller based on H_∞ ($\lambda < 1, \delta < 1$).

6.2. Zero after pole pattern

A collocated plant with zero after pole pattern is considered in Eq. (19). The parameters of this plant are presented in Table 6.

$$G(s) = \frac{s^2 + 0.04*s + 400}{s^2 + 0.02*s + 100} \tag{19}$$

This plant has zero after pole pattern ($\lambda > 1$). For this plant, two NDF controllers (based on H_2 and H_∞) are designed and applied.

Table 6
Parameters of zero after pole system.

ξ_z	0.001
ξ_p	0.001
ω_z	20
ω_p	10
g	1

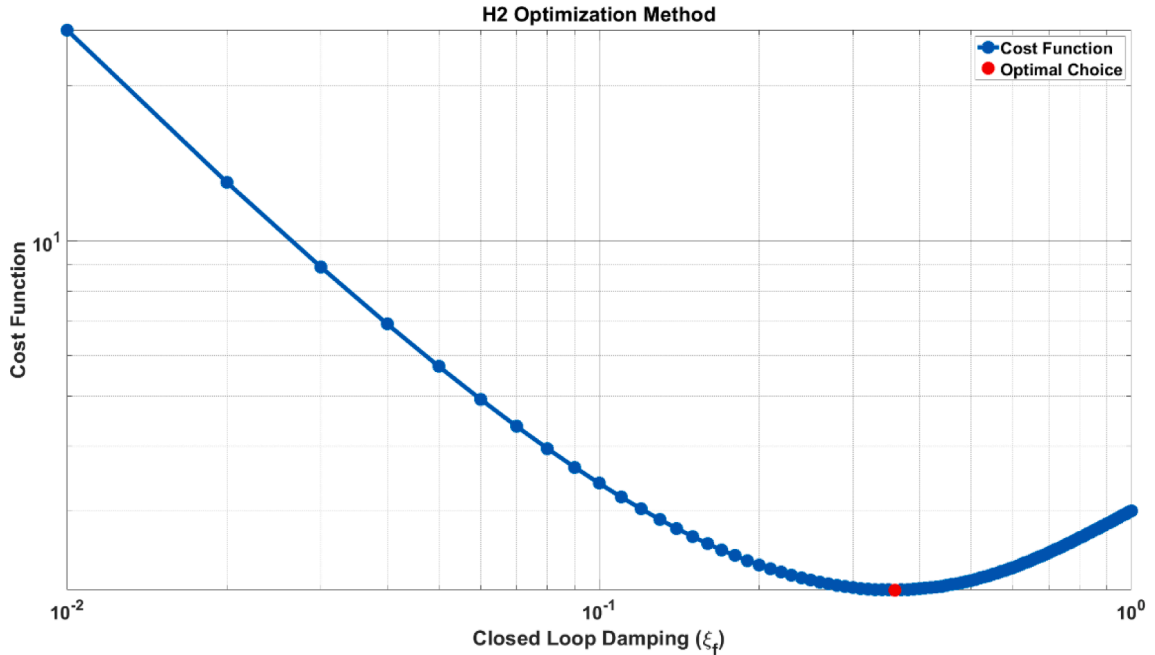


Fig. 10. The cost function of NDF controller based on H_2 for various closed-loop damping ($\lambda > 1$).

Table 7
Values of designed NDF controller (by H_2 & H_∞) with closed-loop damping value (ξ_f) ($\lambda > 1$).

	H_2	H_∞
ξ_f	0.3600	1.0
ξ_c	1.1930	6.1458
ω_c	4.9506	1.7200
K_c	-0.3434	-2.6583

The cost function of NDF controller based on H_2 optimization method for various closed-loop damping (from zero to one) is shown in Fig. 10.

The minimum value of the cost function in Fig. 10 is chosen and considered an optimal choice for NDF controller. After finding the optimal value of closed-loop damping, the NDF controller’s parameters are calculated directly using Table 1. They are presented in Table 7. For the same plant presented in Eq. (19), the cost function of H_∞ method is calculated for various closed-loop damping from zero to one. There is no optimal value in this condition, and the maximum closed-loop possible in this case is one. The parameters of the controller in this condition are also presented in Table 7 as well.

In order to compare H_2 and H_∞ method, their bode diagram are presented in one figure with the open-loop response in the Fig. 11. The root locus of closed-loop system considering H_2 and H_∞ method is also presented in Figs. 12 and 13, respectively.

Obviously, in Fig. 11, H_∞ method can reduce the vibration in the natural frequency more than H_2 method. However, this comes with a price of a higher magnitude of vibration amplification before the natural frequency, which is an unsettling issue. Also, the frequency interval which has vibration amplification in the case of H_∞ is wider than the case of H_2 method. On the other hand, H_2 has an acceptable vibration reduction in the targeted mode with lower vibration amplification at lower frequencies and also in lower frequency interval range. These downsides characteristics of H_∞ method makes H_2 method more appealing, applicable and practical.

Based on Table 6, the plant’s damping without a controller is 0.001 and in Figs. 12 and 13, the damping of the closed-loop system is

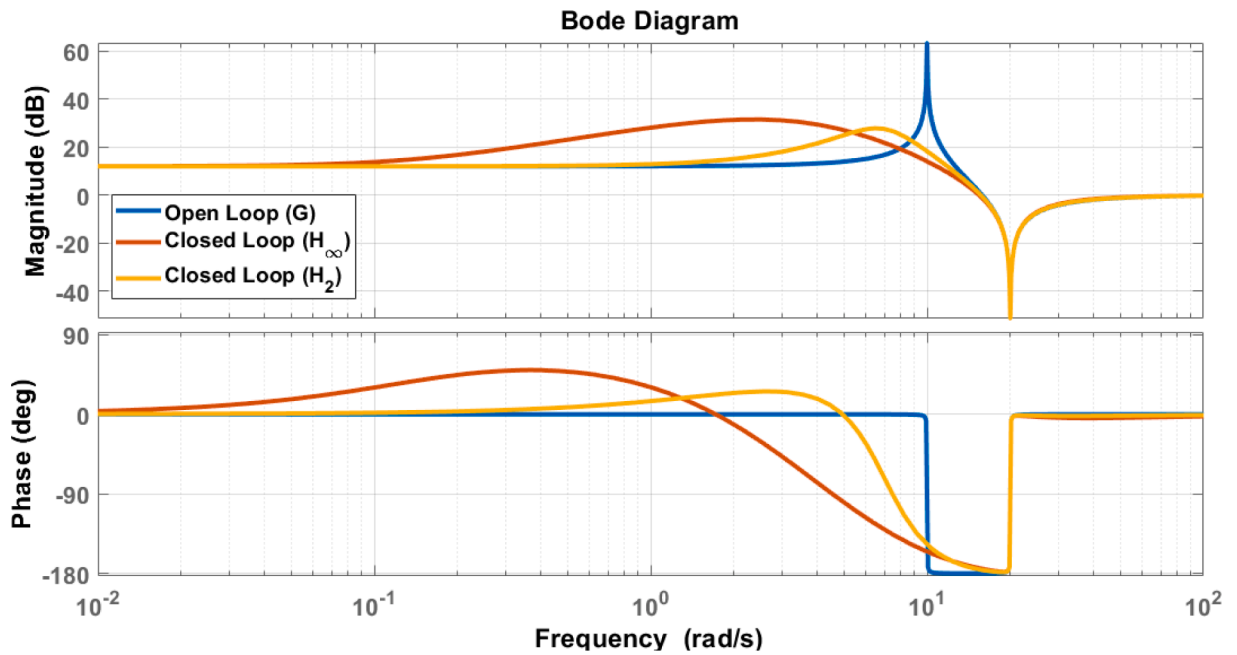


Fig. 11. Open-loop and closed-loop response of the collocated system based on H_2 and H_∞ ($\lambda > 1, \delta < 1$).

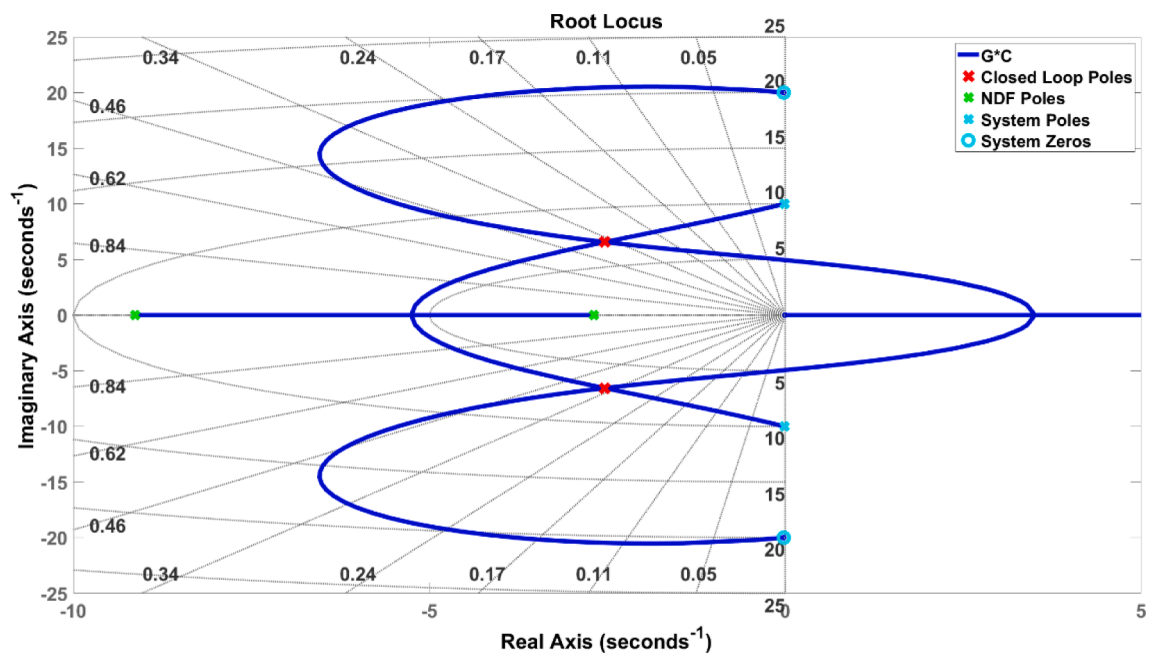


Fig. 12. Root Locus of the collocated system with NDF controller based on H_2 ($\lambda > 1, \delta < 1$).

approximately 0.36 and 1, respectively. This shows a high improvement in damping. This easily shows the power of NDF controller on damping increase of collocated systems with zero after pole pattern (especially low damped systems).

6.3. Robustness

In this section, the robustness of proposed method is evaluated. In this study, closed-loop poles are superimposed in the controller design procedure. This choice can lead to a high sensitivity against coefficient perturbations or uncertainties in the plant. However, since an optimization method like H_2 has been used for finding an optimal choice for closed-loop pole location, the sensitivity against

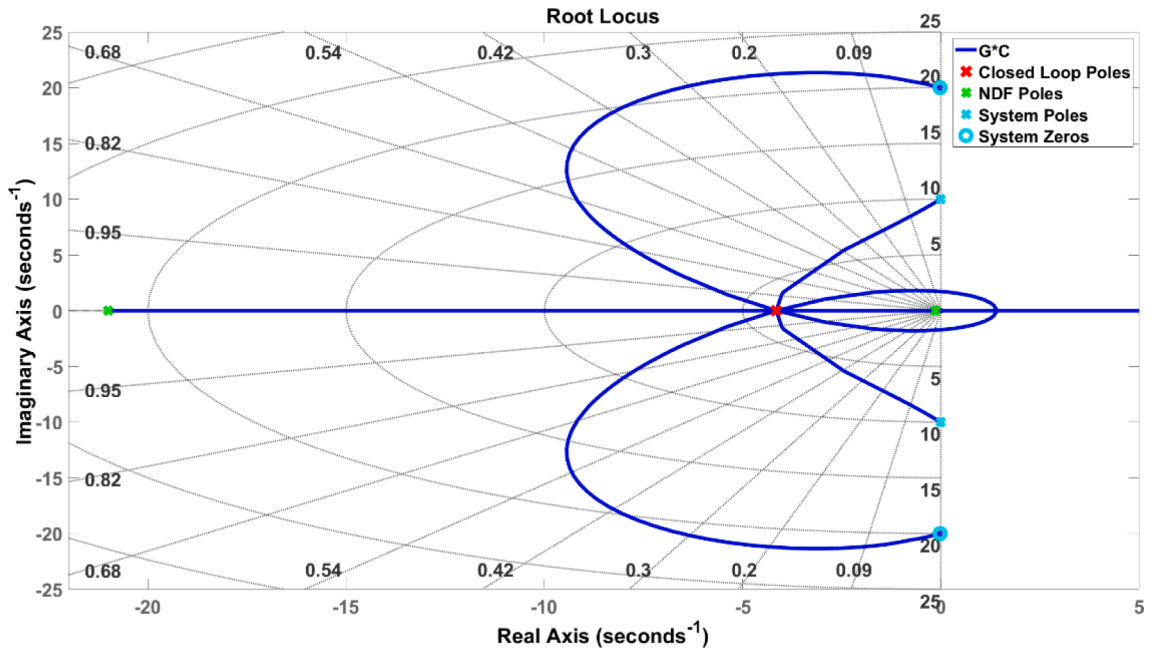


Fig. 13. Root Locus of the collocated system with NDF controller based on H_∞ ($\lambda > 1$, $\delta < 1$).

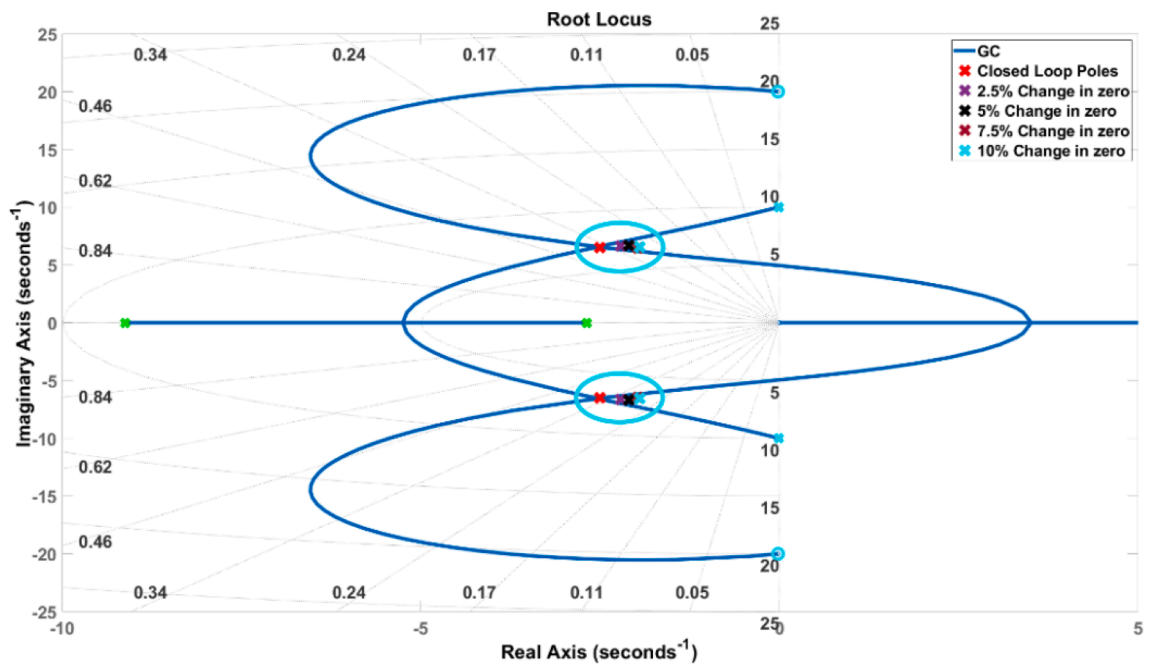


Fig. 14. Root Locus of the collocated system in the case of uncertainties in the zeros of plant.

the coefficient perturbations is decreased. For evaluating this phenomenon, first the plant presented in Eq. (19) and Table 6 is considered. The controller designed by H_2 method for this plant, which is presented in Table 7, is considered. For evaluating the robustness of designed controller, it is considered that the plant's zero changes from zero to 10 percent of its value and the effect of these changes are calculated and presented in Fig. 14.

Clearly, as the location of zero in the plant changes, the closed-loop poles are changing and this leads to decrease in the closed-loop damping value. However, the magnitude of closed-loop damping is not changing a lot. It is decreasing from 0.36 to 0.285 when there is 10 percent change in the location of zero which is not considerable. The same evaluation has been done for pole place change. It is considered that the plant's pole changes from zero to 20 percent of its value and the effect of these changes are calculated and

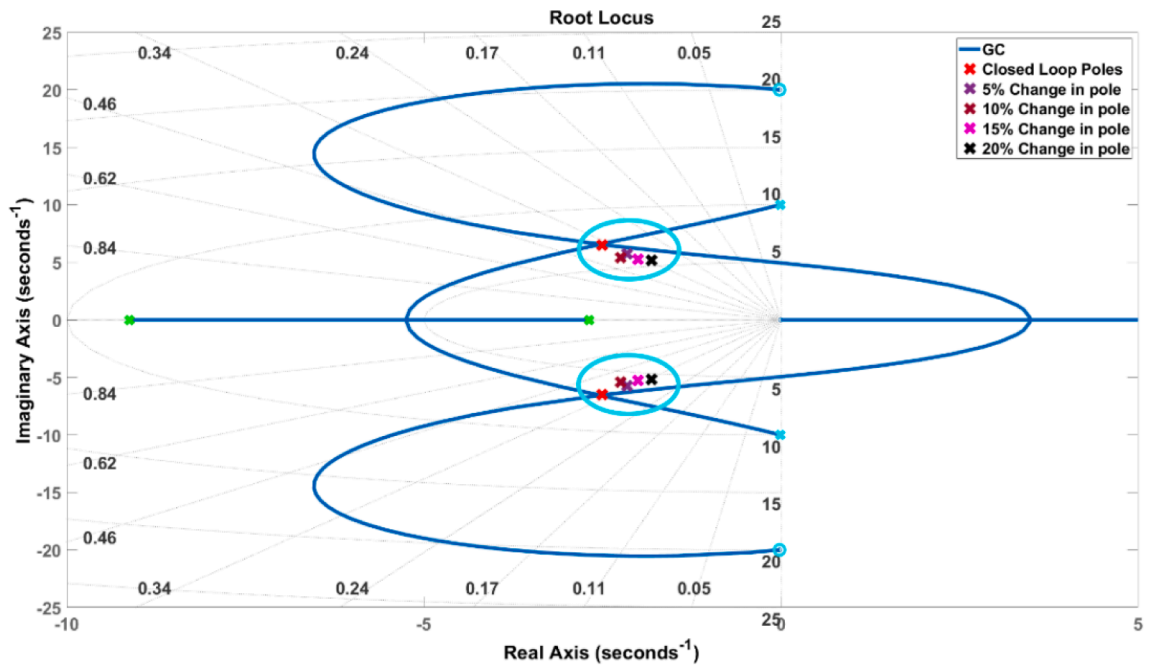
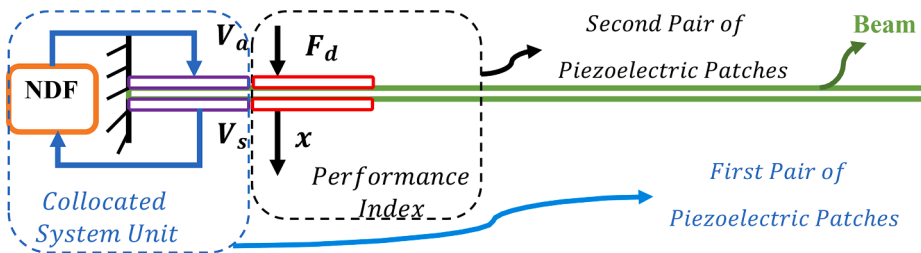
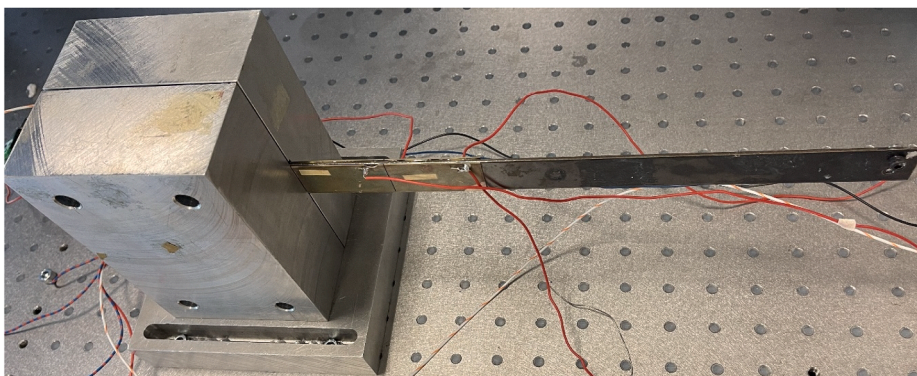


Fig. 15. Root Locus of the collocated system in the case of uncertainties in the poles of plant.



(a)



(b)

Fig. 16. a) Schematic of the cantilever beam and corresponding b) Experimental setup of Cantilever Beam with two pairs of Piezoelectric Patches (the first pair considered for controlling beam and the second for the performance index).

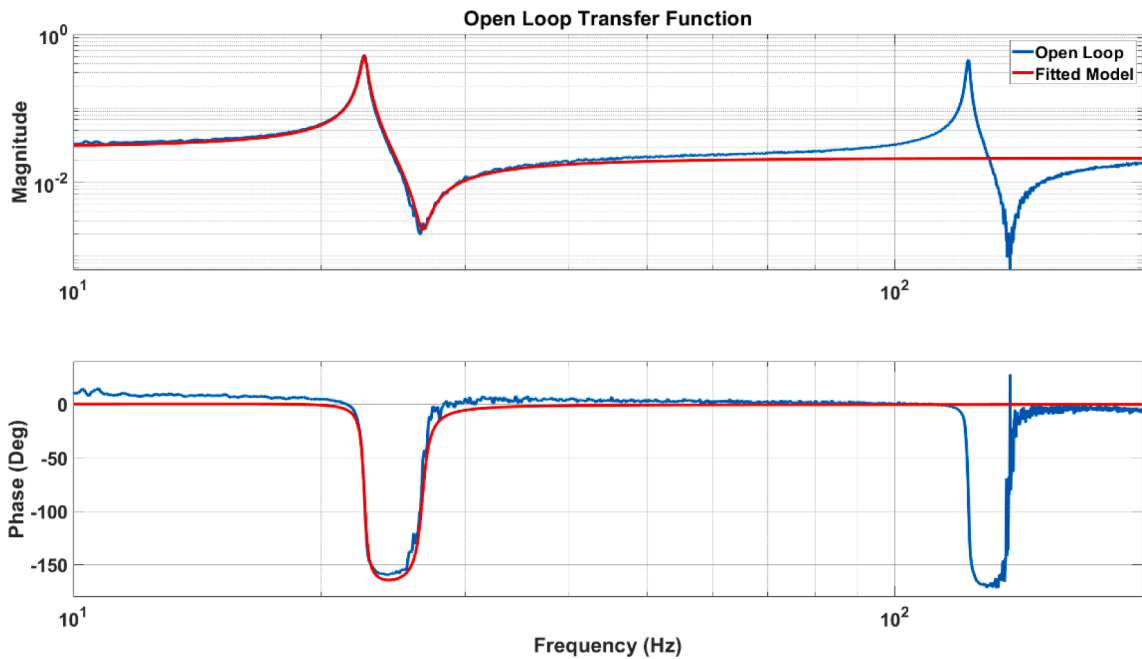


Fig. 17. Open-loop Transfer Function with Fitted Model.

presented in Fig. 15.

In this condition, the closed-loop damping value is much less sensitive to the changes of pole in the plant. As the plant's pole changes from zero to 20 percent of its value, the closed-loop damping value decreases from 0.36 to 0.33 which is less than previous condition. This means that in this condition, the controller is less sensitive (or more robust) against the changes in the pole location's uncertainties.

7. Experimental validation

In this section, a detailed experiment is presented to validate the proposed algorithm for designing NDF filter experimentally. To this end, the first mode of a cantilever beam is targeted. The beam has two pairs of piezoelectric patches. The first pair of piezoelectric patches are used for the controlling unit, and the second pair is utilized to measure the performance index of the beam before and after applying the controller (Fig. 16). The transfer function between the actuator and sensor is collocated due to the same position of patches along the beam.

In the following section, the transfer function between actuator and sensor is estimated first and considered as a plant. Then, the optimal NDF control for the estimated transfer function is designed. Finally, the designed controller is applied to the structure experimentally and the results are compared with the uncontrolled conditions. The optimal NDF is also compared with an optimized PPF experimentally as well, as an experimental comparison of NDF and PPF.

7.1. The Open-Loop transfer function

A schematic of the cantilever beam and its corresponding experimental setup are shown in Fig. 16a and b, respectively. The length, width, and thickness of beam, which is made of steel, are 255 mm, 30 mm, and 3 mm respectively. Piezoelectric patches No.1, 2, 3, and 4 are standard PIC-225 patches, glued on each side of the beam as shown in Fig. 14. The cantilever beam has two pairs of piezoelectric patches and the first one is considered a controlling unit. The second pair is used to measure the performance index of the beam. The first step of the experiment is extracting the transfer function of the collocated plant. For this purpose, MicroLab-Box is used to inject the excitation signal into the actuator and measure the sensor signal from the setup at a sampling frequency of 10 kHz. By this method, the frequency response between actuator and sensor is extracted experimentally. The aim of this experiment is to damp the first mode of the beam. Therefore, in the open-loop extracted from the actuator to the sensor, a model has been fitted to the first mode of beam. In other words, the model of interest has been obtained based on transfer function estimation in MATLAB by fitting a collocated transfer function to experimental frequency response around the first mode shown in Fig. 17. The pole-zero pattern in this plant is pole before zero.

The transfer function of the fitted model is presented in Eq. (20). This transfer function is used in the procedure of designing the controller.

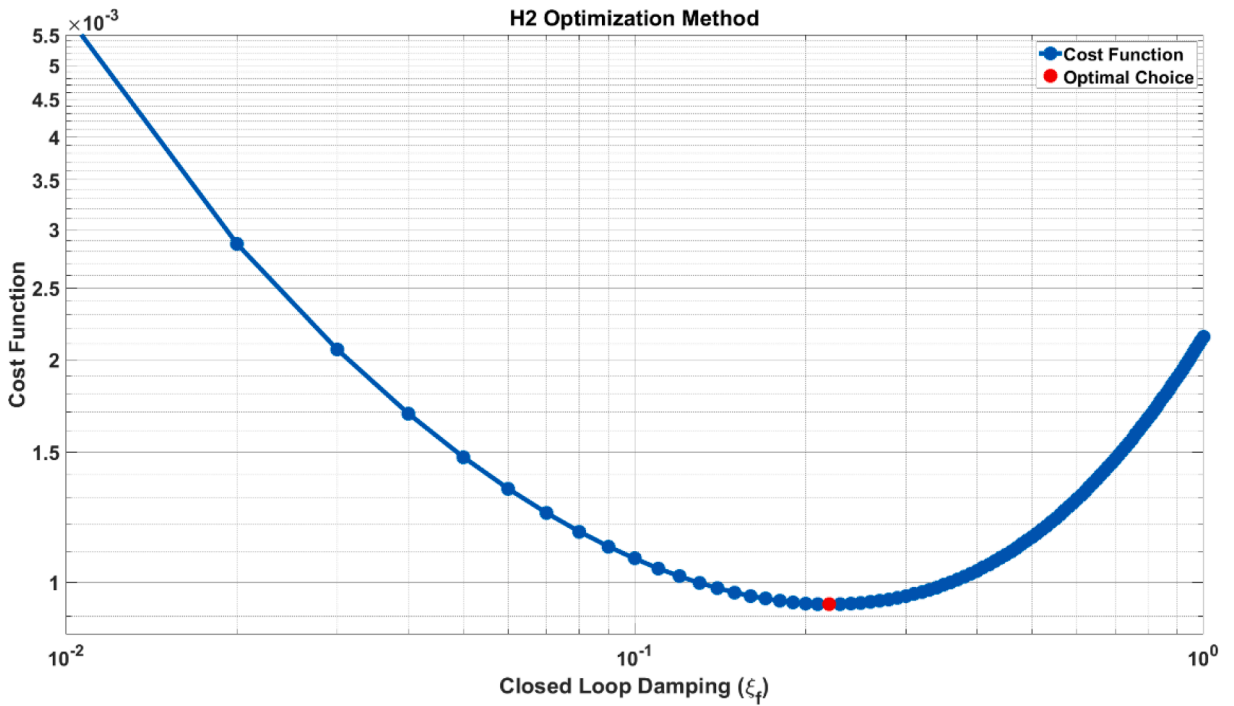


Fig. 18. The cost function of NDF controller based on H_2 for various closed-loop damping ($\lambda > 1$).

Table 8
 Values of designed NDF controller (by H_2) with closed-loop damping value (ξ_f).

Method	H_2
ξ_f	0.2100
ξ_c	0.9999
ω_c	93.0054
K_c	-395.8480

$$G(s) = 0.0212 \frac{s^2 + 5.0142s + 2.7934e4}{s^2 + 2.272s + 2.016e4} \tag{20}$$

7.2. Optimal NDF design

After extracting the model, an optimal NDF filter is designed based on it. For optimization, H_2 method is utilized and its cost function for different values of closed-loop damping is presented in Fig. 18.

The minimum value of the cost function in Fig. 18 is chosen and considered an optimal choice for NDF controller. Afterward, the parameters of NDF filter are calculated and presented in Table 8 accordingly.

The optimal NDF is applied to the model and the bode diagram and root locus diagram of closed-loop system are presented in Fig. 19 and Fig. 20, respectively.

Based on Eq. (20), the structure’s damping in the first mode is 0.0047. In Fig. 20, the damping of closed-loop system is 0.21, which shows a high improvement in system’s damping by closing the loop.

7.3. PPF design

For showing the impact of NDF more clearly, the performance of NDF has been compared with the Positive Position Feedback (PPF) filter, which is a very popular controller for increasing the damping of one mode. PPF is one of the most attractive vibration control methods due to its stability and ease of implementation. For designing PPF optimally, an algorithm based on maximum damping and H_2 presented in [6] is used for the fitted model (Eq. (20)). The PPF is applied to the model and the bode diagram and root locus diagram of closed-loop system are presented in Figs. 21 and 22, respectively.

Based on Fig. 22, PPF can damp the first mode and closed-loop damping considering this technique will be 0.1058 which is

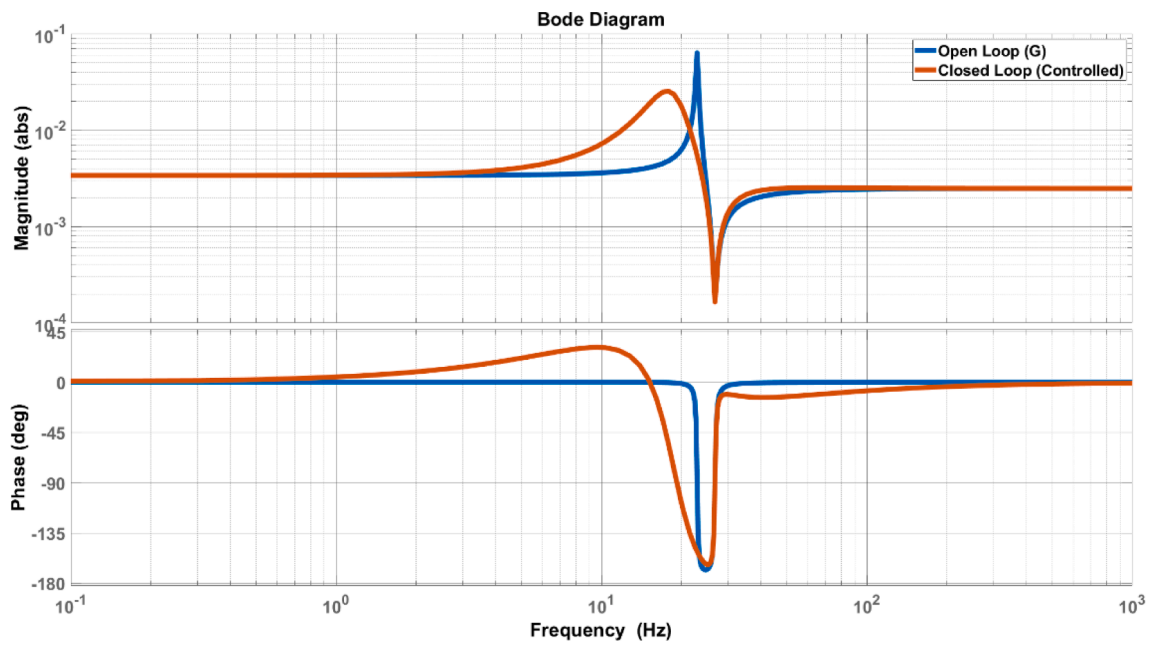


Fig. 19. Open-loop and closed-loop response of the fitted model with optimal NDF controller.

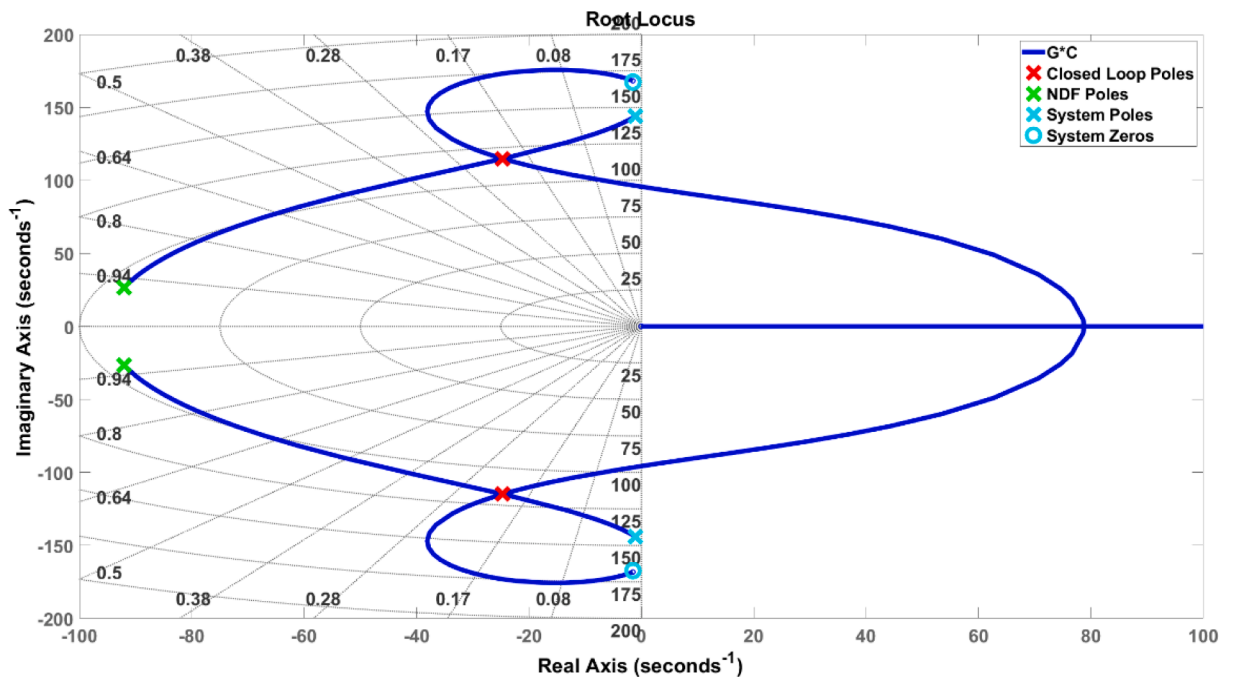


Fig. 20. Root Locus of the fitted model with NDF controller ($\lambda > 1$, $\delta < 1$).

approximately half of the magnitude of closed-loop damping of the system with the designed NDF filter.

7.4. Applying designed controllers

After designing optimal NDF and PPF controllers for the fitted model, in this section, both controllers are applied on the cantilever beam experimentally. The controller is used to close the loop of the collocated plant. The performance index of the structure is extracted by the second pair of piezoelectric patches in both of uncontrolled condition and controlled conditions with NDF and PPF

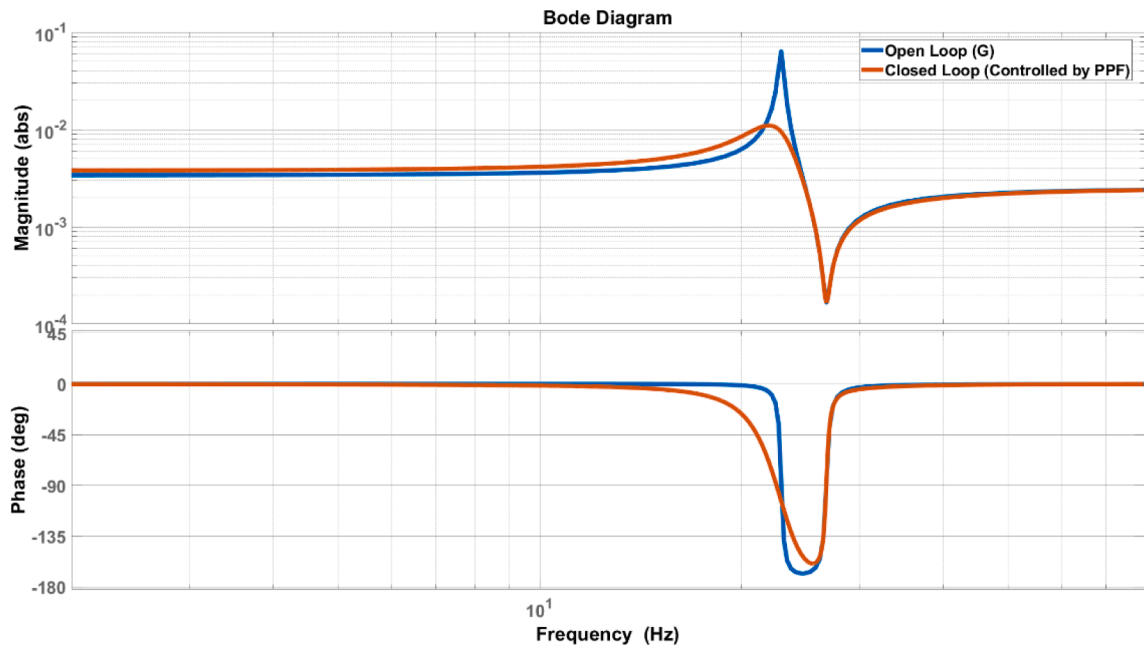


Fig. 21. Open-loop and closed-loop response of system by PPF controller.

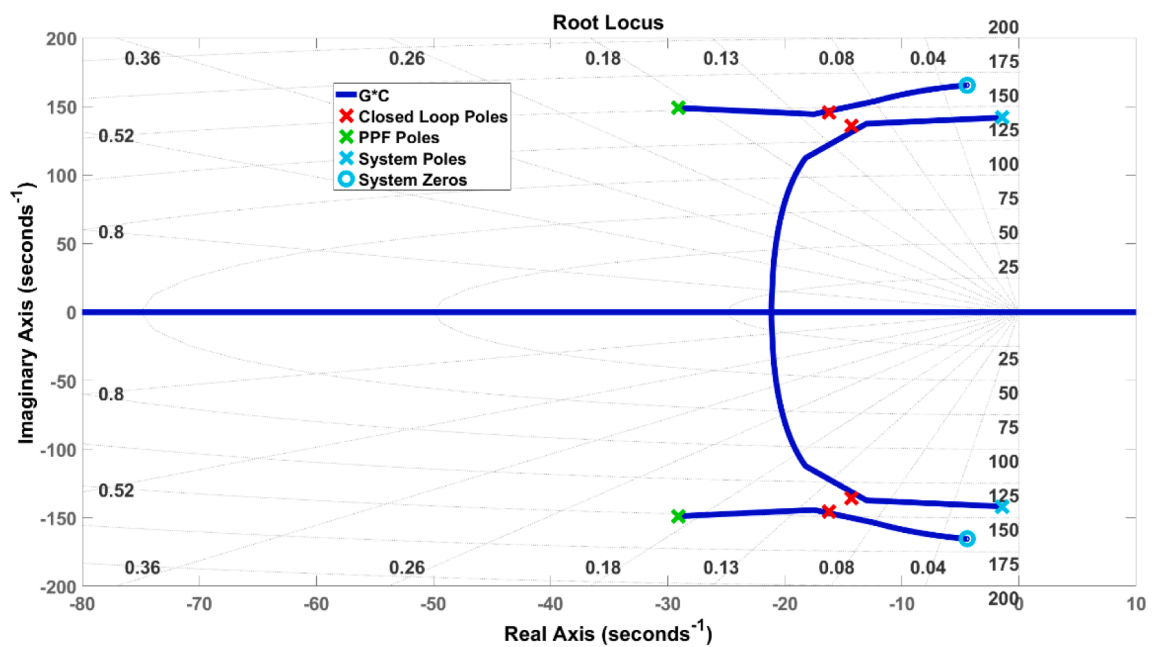


Fig. 22. Root Locus of the experimental setup with PPF controller.

controllers. The results are presented in Fig. 23.

As it is shown in Fig. 23, the PPF controller can damp the targeted mode (first mode) admissibly. The PPF controller does not have any effects in other modes and obviously, in the second and third mode, there are no added damping to the beam using PPF controller. So, in overall, PPF can only damp the targeted mode with an acceptable amount of vibration reduction.

On the other hand, NDF controller can powerfully damp the targeted mode (first mode) easily. Clearly, the level of vibration attenuation in the first mode, in this case, is higher than PPF. So, only considering the first mode, the results show that NDF not only can reduce a high amount of vibration but also it can easily outperform the performance of PPF controller in terms of vibration attenuation.

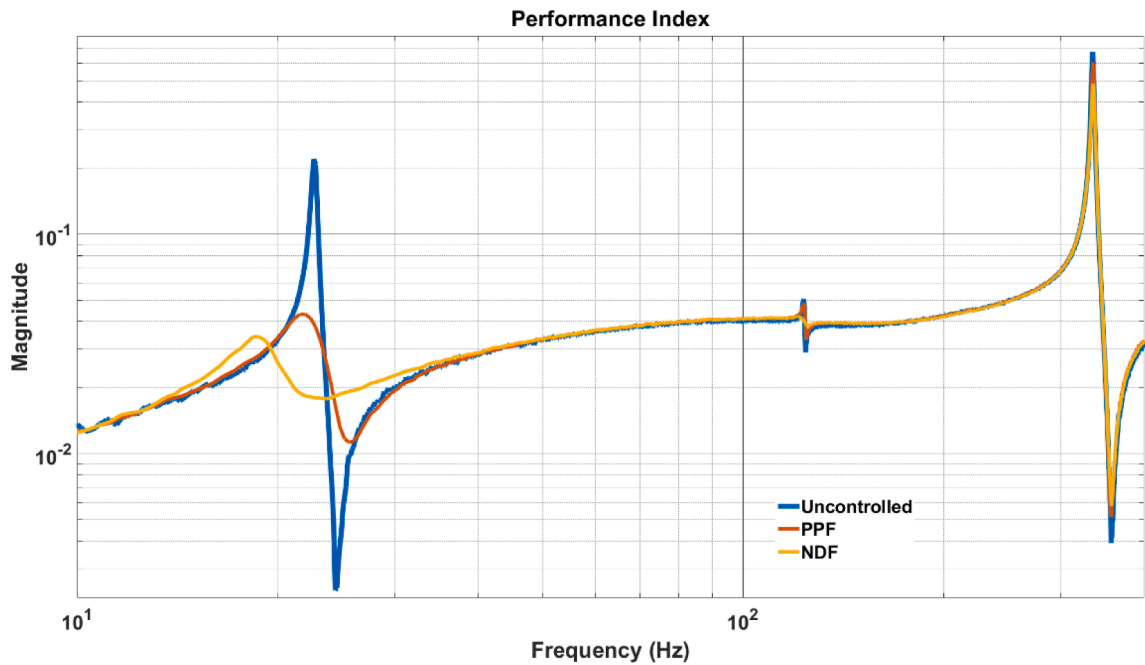


Fig. 23. Performance Index of Beam (Frequency Response between second pair of Piezoelectric Patches) in uncontrolled condition and with PPF, NDF controller.

Besides, even though the NDF is designed for the first mode, it has increased the damping of the beam in the second and third modes of the beam as well. In Fig. 22, the second mode is damped completely and in the third mode, there is a minor vibration reduction using NDF controller. This shows the high power and impact of the NDF on vibration reduction. Since the NDF controller is a band-pass filter which means that it works only in a bandwidth of frequency and the modes which are in this bandwidth of frequency will be affected by applying NDF controller. The effect of NDF controller is the highest in the modes which are in the vicinity of the targeted mode (modes after the target mode) and as the distance of modes increases from the targeted mode, the effect of NDF decreases in those modes. For instance, in Fig. 22, the second mode is more affected (damped) by NDF controller in comparison with the third mode, due to the closeness to the first mode (targeted mode). The only downside of NDF filter is slight vibration magnification before the targeted mode. However, overall, the NDF filter is very powerful in vibration mitigation applications in comparison with other controllers.

In overall, NDF can outperform PPF in terms of performance in the targeted mode and it can create more damping in the structure. Also, NDF can damp the modes in the vicinity of the targeted mode as well, in which PPF does not have any performance. Therefore, it can be concluded that not only NDF is a powerful filter to damp the vibration of the beam but also it can easily outperform PPF filter in terms of vibration attenuation. Therefore, NDF has more power than PPF in increasing damping in the structure and it can work in a band of frequency, in overall.

8. Conclusion

In this article, a procedure for designing NDF filter for the collocated systems based on maximum damping and H_2 or H_∞ method is presented. NDF controller, as a band-pass filter, can effectively eliminate the lower and higher frequency disturbances. A simple, collocated system is considered and a mode of this system is targeted to damp. The Maximum damping method is used to determine all of the controller's parameters dependent on the closed-loop damping value. Afterward, H_2 or H_∞ method is utilized to determine the closed-loop damping value, optimally. The results show that NDF not only can easily damp a targeted mode powerfully but also can reduce some level of vibrations in the modes in the vicinity of the targeted mode as well without any destabilizing issues. This shows the power of NDF filter on vibration mitigation of a band of frequency. The interesting point is that this method has no restrictions for application and it is applicable for any collocated system with zero before pole pattern or zero after pole pattern. Also, it has shown that the NDF filter can outperform the PPF controller in terms of performance on the targeted mode and even in the modes in the vicinity of the targeted mode.

Declaration of Competing Interest

The authors declare that they have no known competing financial interests or personal relationships that could have appeared to influence the work reported in this paper.

Acknowledgements

The authors gratefully acknowledge the Walloon Region for funding this research. The work has been done in the frame of the MAVERIC project (grant agreement number 1610122).

References

- [1] A. Preumont, *Vibration Control of Active Structures*, Kluwer academic publishers, Dordrecht, 1997 Jan.
- [2] M.J. Balas, Direct velocity feedback control of large space structures, *J. Guid. Control Dynam.* 2 (3) (1979) 252–253, <https://doi.org/10.2514/3.55869>.
- [3] A. Preumont, J.-P. Dufour, C. Malekian, Active damping by a local force feedback with piezoelectric actuators, *J. Guid. Control. Dyn.* 15 (2) (1992) 390–395, <https://doi.org/10.2514/3.20848>.
- [4] Fleming AJ, Behrens S, Moheimani SO. A new approach to piezoelectric shunt damping. InProc. Int. Symp. Smart Structures and Microsystems.
- [5] J.L. Fanson, An Experimental Investigation of Vibration Suppression in Large Space Structures Using Positive Position Feedback, Phd thesis, California Institute of Technology, 1987. 10.7907/0SA8-HW86.
- [6] Ahmad Paknejad, Gouying Zhao, Michel Osee, Arnaud Deraemaeker, Frederic Robert and Christophe Collette, A novel design of positive position feedback controller based on maximum damping and optimization, *Journal of Vibration and Control*, 2020, Vol. 26(15–16) 1155–1164. <https://doi.org/10.1177%2F1077546319892755>.
- [7] S. O. Reza Moheimani, Benjamin J. G. Vautier, Bharath Bhikkaji, “Experimental Implementation of Extended Multivariable PPF Control on an Active Structure” IEEE TRANSACTIONS ON CONTROL SYSTEMS TECHNOLOGY, VOL. 14, NO. 3, MAY 2006. <https://doi.org/10.1109/TCST.2006.872532>.
- [8] C. Collette, S. Chesné, Robust hybrid mass damper, *J. Sound Vib.* 375 (4) (2016) 19–27, <https://doi.org/10.1016/j.jsv.2016.04.030>.
- [9] G. Zhao, A. Paknejad, A. Deraemaeker, C. Collette, “ optimization of an integral force feedback controller”, *Journal of Vibration and control*, Vol 25, Issue 17, 2019. <https://doi.org/10.1177%2F1077546319853165>.
- [10] G. Cazzulani, F. Resta, F. Ripamonti, R. Zanzi, Negative derivative feedback for vibration control of flexible structures, *Smart Mater. Struct.* (2012) 10, <https://doi.org/10.1088/0964-1726/21/7/075024>, 075024.
- [11] F. Cola, F. Resta, F. Ripamonti, A negative derivative feedback design algorithm, *Smart Mater. Struct.* 10 (2014), <https://doi.org/10.1088/0964-1726/23/8/085008>, 085008.
- [12] Hassaan Hussain Syed “Comparative study between positive position feedback and negative derivative feedback for vibration control of a flexible arm featuring piezoelectric actuator” *International Journal of Advanced Robotic Systems*, (2017) (1-9). <https://doi.org/10.1177%2F1729881417718801>.
- [13] F Ripamonti and F Cola, “Control system for a carbon fiber plate using an adaptive negative derivative feedback control algorithm” *Journal of Vibration and Control*, 2018, Vol. 24(21) 4988–4999. <https://doi.org/10.1177%2F1077546317740451>.
- [14] N. Debattisti, M.L. Bacci, S. Cinquemani, Distributed wireless-based control strategy through Selective Negative Derivative Feedback algorithm, *Mech. Syst. Sig. Process.* 142 (2020) 106742.
- [15] R. Jamshidi, A.A. Jafari, Conical shell vibration control with distributed piezoelectric sensor and actuator layer, *Compos. Struct.* 256 (2021) 113107.
- [16] R Jamshidi, A Jafari. Nonlinear vibration of conical shell with a piezoelectric sensor patch and a piezoelectric actuator patch. 2021, *Journal of Vibration and Control*, 1077546321996922. <https://doi.org/10.1177%2F1077546321996922>.
- [17] R. Jamshidi, A. Jafari, Conical shell vibration optimal control with distributed piezoelectric sensor and actuator layers, *ISA Trans.* 117 (2021) 96–117.
- [18] R. Jamshidi, A. Jafari, Evaluating sensor distribution in simply supported truncated conical shells with piezoelectric layers, *Mech. Adv. Mater. Struct.* 26 (14) (2018) 1179–1194, <https://doi.org/10.1080/15376494.2018.1432791>.
- [19] R. Jamshidi, A. Jafari, Transverse sensing of simply supported truncated conical shells, *J. Comput. Appl. Mech.* 49 (2) (2018) 212–230, <https://doi.org/10.22059/jcmech.2017.238393.167>.
- [20] R. Jamshidi, A. Jafari, Evaluating actuator distributions in simply supported truncated thin conical shell with embedded piezoelectric layers, *J. Intell. Mater. Syst. Struct.* 29 (12) (2019) 2641–2659, doi: 10.1177%2F1045389X18770905.
- [21] B. Bao, D. Guyomar, M. Lallart, Vibration reduction for smart periodic structures via periodic piezoelectric arrays with nonlinear interleaved-switched electronic networks, *Mech. Syst. Sig. Process.* 82 (1) (2017) 230–259, <https://doi.org/10.1016/j.ymssp.2016.05.021>.
- [22] O. Thomas, J. Ducarne, J.-F. Deü, Performance of piezoelectric shunts for vibration reduction, *Smart Mater.* 21 (2012), <https://doi.org/10.1088/0964-1726/21/1/015008>, 015008.
- [23] G. Raze, A. Jadoul, S. Guichaux, V. Broun, G. Kerschen, A digital nonlinear piezoelectric tuned vibration absorber, *Smart Mater. Struct.* 29 (1) (2020) 015007.
- [24] G. Raze, S. Guichaux, A. Jadoul, V. Broun, G. Kerschen, A digital absorber for nonlinear vibration mitigation, *Nonlinear Struct. Syst.* 1 (2021) 105–108, https://doi.org/10.1007/978-3-030-47626-7_16.
- [25] I. Giorgio A. Culla D. Del Vescovo Multimode vibration control using several piezoelectric transducers shunted with a multiterminal network *Archive of Applied Mechanics* 79 9 2009 859 879 <https://hal.archives-ouvertes.fr/hal-00798627>.
- [26] D. Williams, H. Haddad Khodaparast, S. Jiffri, C. Yang, Active vibration control using piezoelectric actuators employing practical components, *J. Vib. Control* 25 (21-22) (2019) 2784–2798.
- [27] M.A. Trindade, A. Benjeddou, R. Ohayon, Piezoelectric active vibration control of damped sandwich beams, *J. Sound Vib.* 246 (4) (2001) 653–677.
- [28] J. Li, Y.u. Xue, F. Li, Y. Narita, Active vibration control of functionally graded piezoelectric material plate, *Compos. Struct.* 207 (2019) 509–518.
- [29] Takayoshi Kamada, Takafumi Fujita, Takayoshi Hatayama, Takeo Arikabe, Nobuyoshi Murai, Satoru Aizawa and Kohtarō Tohyama. “Active vibration control of frame structures with smart structures using piezoelectric actuators (Vibration control by control of bending moments of columns)” 1997 *Smart Mater. Struct.* 6 448. <https://doi.org/10.1088/0964-1726/6/4/009>.
- [30] S. Nima Mahmoodi, M. Ahmadian, Modified acceleration feedback for active vibration control of aerospace structures, *Smart Mater. Struct.* 19 (6) (2010) 065015.
- [31] P.u. Yuxue, H. Zhou, Z. Meng, Multi-channel adaptive active vibration control of piezoelectric smart plate with online secondary path modelling using PZT patches, *Mech. Syst. Sig. Process.* 120 (1) (2019) 166–179, <https://doi.org/10.1016/j.ymssp.2018.10.019>.
- [32] Giorgio, I., Del Vescovo, D. Energy-based trajectory tracking and vibration control for multilink highly flexible manipulators. *Mathematics and Mechanics of Complex Systems*, 7(2), 159-174. <https://doi.org/10.2140/memocs.2019.7.159>.